J Solid State Eletrochem (2004) 8: 538–543
DOI 10.1007/s10008-003-0481-x

ORIGINAL PAPER

Ping Wu · Chenxin Cai

The solid state electrochemistry of samarium (III) hexacyanoferrate (II)

Received: 6 October 2003 / Accepted: 11 November 2003 / Published online: 24 January 2004

Abstract A new electroactive polynuclear inorganic compound of a rare earth metal hexacyanoferrate, samarium hexacyanoferrate (SmHCF), was prepared chemically and characterized using techniques of FTIR spectroscopy, thermogravimetric analysis (TGA), X-ray powder diffraction, UV–Vis spectrometry and X-ray photoelectron spectroscopy (XPS) etc. The cyclic voltammetric behavior of SmHCF mechanically attached to the surface of graphite electrode was well defined and exhibited a pair of redox peaks with the formal potential of 180.5 mV (versus SCE) at a scan rate of 100 mV/s in 0.2-M NaCl solution and the redox peak currents increased linearly with the square root of the scan rates up to as high as 1,000 mV/s. The effects of the concentration of supporting electrolyte on the electrochemical characteristics of SmHCF and the transport behavior of K^+, Na^+ and Li^+ counter-ions through the ion channel of SmHCF were studied by voltammetry.

Keywords Cyclic voltammetry · Chemically modified electrode · Solid state electrochemistry · Samarium hexacyanoferrate

Introduction

Ever since the pioneering work of Neff [1] and Itaya et al. [2], Prussian blue (PB) and related metal cyanometalate compounds, which belong to a class of polynuclear inorganic compounds and resemble not only redox organic polymers, but also zeolitic or intercalation materials, have been studied extensively. There have been many papers published over the years on the preparation and characterization of metal haxacyanoferrates as electroactive materials [3, 4, 5, 6, 7, 8, 9, 10, 11, 12, 13, 14, 15, 16, 17, 18, 19, 20] because they possess intriguing properties, such as electrochromicity [21, 22], capability to store counter-cations [23, 24], ion-exchange selectivity [25], ability to mediate electrochemical reactions [10, 11, 20, 26, 27, 28, 29, 30, 31, 32] and molecular magnetism [33, 34] etc.

Although there are considerable reports about the preparation and characteristics of the transition metal hexacyanoferrates as well as their applications, only one paper, to our knowledge, reported the electrochemical preparation and characterization of rare earth metal hexacyanoferrates, lanthanum hexacyanoferrate [4]. Rare earth metals (or ions) have been received much attention in many fields, such as in the hydrogen storage materials of batteries [35], ion selective electrodes and chemical sensors [36], electrocatalytic hydrogenation of organic substrates [37] and as a promoter to facilitate the electrochemical reaction of biological molecules, for example microperoxidase-11 [38]. In our previous manuscript [39], a new rare earth metal hexacyanoferrate, samarium hexacyanoferrate (SmHCF), was prepared electrochemically by a procedure of potential cycling and was characterized by cyclic voltammetry and scanning electron microscopy (SEM). In this work, SmHCF was prepared chemically and characterized by techniques of FTIR spectroscopy, thermogravimetric analysis (TGA), X-ray powder diffraction, UV–Vis spectrometry and X-ray photoelectron spectroscopy (XPS) etc. The electrochemical characteristics of the SmHCF were studied by solid state electrochemistry (voltammetry of immobilized microparticles) [40, 41]. In contrast to previous electrochemical studies of metal hexacyanoferrates, which were generally formed as a thin film on the surface of electrode, SmHCF was mechanically attached to the surface of graphite electrode using a technique initially developed by Scholz and co-workers [42, 43]. The method of solid state electrochemistry provides an array of microcrystalline particles

P. Wu · C. Cai (✉)
Department of Chemistry,
Nanjing Normal University,
210097 Nanjing, P.R. China
E-mail: caichenxiin@njnu.edu.cn
Tel.: +86 25 83598031
Fax: +86 25 83598448

of SmHCF on the surface of the electrode rather than forming a thin film, thus a large range of solid and insoluble materials may be investigated electrochemically. Furthermore, the study of the electrochemistry of solid hexacyanoferrates is very important to gain access to the fundamentals of solid state electrochemistry [40].

Experimental

Chemicals

Samarium chloride hexahydrate (99 + %, Aldrich) was used without further purification. All other chemicals were of analytical grade and were used as received. All solutions were prepared with doubly distilled water.

Preparation of samples

The following samarium (III) hexacyanoferrate (II) samples: $NaSmFe(CN)_6{\cdot}3H_2O$, $KSmFe(CN)_6{\cdot}3H_2O$ and $LiSmFe(CN)_6{\cdot}3H_2O$ were prepared by precipitation via dropwise addition of 100 ml of 20-mM $SmCl_3$ into a stirred solution of 100 ml of 20-mM $Na_4Fe(CN)_6$ (each containing NaCl, KCl or LiCl, respectively, at 1-M level). The resulting precipitates were filtered off and washed: first, with the respective NaCl, KCl or LiCl electrolyte, respectively, and later, with distilled water. The three prepared compounds have a similar color of pale yellow and the peaks of the three compounds are located at 405 nm in UV–Vis spectra. The composition of sample, for example $NaSmFe(CN)_6$, was calculated to be $Na_{1.0015}Sm_{0.9995}Fe(CN)_6$ by chemical analysis of the content Fe, Sm and Na (K or Li) in the samples. The calculated stoichiometry of the samples is very closed to the theoretical one. All the solid samples were dried for overnight in vacuum at ambient temperature and stored in a desiccator.

Apparatus

Fourier transform infrared (FTIR) spectra of SmHCF were recorded on KBr disk using a Nexus 670 FT-IR spectrophotometer (Nicolet Instrumental Co., USA). For each sample, a total of 64 scans at a resolution of 4 cm^{-1} were used. The X-ray diffraction (XRD) experiments were performed with a Shimadzu XD-3A X-ray diffractometer (Japan) using Cu-K_α radiation ($\lambda = 0.15418$ nm). The scan rate was 4°/min. The thermogravimetric analysis (TGA) of the samples was performed by the 7 Series Thermal Analysis System (Perkin Elmer). The rate is 10 K/min. The iron, samarium and sodium (potassium or lithium) content of all samples was determined by inductively coupled plasma (ICP) atomic emission spectroscopy (PS-I, Leeman) of the digested samples. Digestion was achieved by hydrochloric acid. The UV–Vis spectra of SmHCF were obtained using a Hitachi U-3400 spectrophotometer (Japan). XPS experiments were carried out on ESCALab MK2 using monochromatic Mg K_α line at 1253.6 eV. The values of binding energy were calibrated with that of C 1s (284.6 eV).

The electrochemical experiments were performed with a CHI 600 electrochemical workstation (CH Instruments, USA) and a three-electrode electrochemical cell. A coiled Pt wire and a saturated calomel electrode (SCE) were used as the counter-electrode and the reference electrode, respectively. The working electrode used in this study was a paraffin-impregnated graphite electrode, which was prepared and impregnated using commercial graphite rods (spectroscopically pure) in this laboratory. Solid samples of SmHCF were mechanically attached to the surface of electrode as follows [43]: about 2 mg of $NaSmFe(CN)_6{\cdot}3H_2O$, $KSmFe(CN)_6{\cdot}3H_2O$ or $LiSmFe(CN)_6{\cdot}3H_2O$ powder were placed on a piece of weight paper and the electrode was gently rubbed over the samples to make some of the compound adhere to the electrode surface. The surface of graphite electrode can be renewed after each experiment by rubbing the electrode surface on a clean abrasive.

Before the electrochemical experiments, high purity nitrogen was purged into solution for 15 min and a continuous flow of the gas was maintained over the solution during the experiments. The experiments were performed at a room temperature (22 ± 2 °C).

Results and discussion

Characterization of the samples

Figure 1 shows FTIR spectra of SmHCF samples. From the spectra, one can see that the characteristics and the locations of peaks of three spectra are similar. The very strong and sharp peak, which is located at 2,062 cm^{-1} for all samples, can be assigned to the stretching vibration of the C ≡ N group in the SmHCF, because metal hexacyanoferrates, such as Prussian blue and its analogs, have a common characteristic absorption peak around 2,100 cm^{-1}, which corresponds to the stretching vibration of the C ≡ N group [44]. It should be noted that the FTIR peak corresponding to the stretching vibration of C ≡ N group in SmHCF does not split off, which differs from that for CoHCF [13, 45]. The FTIR peak of the stretching vibration of C ≡ N group in CoHCF splits off two peaks because there are two stoichiometric compound existing in the CoHCF system, the ratio of Co to Fe is 1.5 and 1.0, respectively. These results indicate that there is only one stoichiometric compound existing in the SmHCF system. This conclusion is verified by the results of XRD of samples and also consistent with the cyclic voltammetric results, because only one pair of redox peaks appears on the cyclic voltammogram of SmHCF (see later). The peaks at 1,654 and 1,594 cm^{-1} are assigned to the bending vibrations of crystal water contained in the structure of SmHCF samples. The number of crystal water can be calculated to be three from the data of TGA (Fig. 2).

Figure 3 presents the XRD patterns of three SmHCF samples. The XRD patterns for all samples are almost the same, indicating that they have the same symmetry. The major peaks are in very good agreement with the values of potassium iron samarium cyanide hydrate

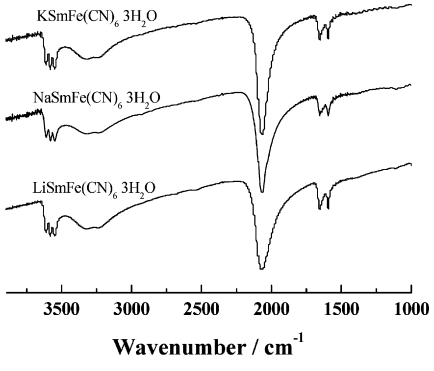

Fig. 1 FTIR spectra of SmHCF

previously reported ($SmKFe(CN)_6{\cdot}3H_2O$, JCPDS card, file 40-755). There is no indication that the samples contain any appreciable amounts of amorphous compounds. Assuming that the three prepared SmHCF compounds have the same monoclinic symmetry as that of $SmKFe(CN)_6{\cdot}3H_2O$ (JCPDS card, file 40-755), one can calculate the lattice parameters of the three SmHCF compounds. Those parameters are presented in Table 1. The lattice parameter of $SmKFe(CN)_6{\cdot}3H_2O$ reported in the literature (obtained from JCPDS card, file of 40-755) is also listed in Table 1 for comparison. The data of Table 1 indicate that the lattice parameters of SmHCF compounds are almost independent on the counter-ions and also almost in agreement with that reported in literature, taking into account the experimental deviation.

The oxidation state of iron and samarium in SmHCF as prepared was determined by the XPS technique. Figure 4 presents the XPS spectra of the Fe 2p region (A) and the Sm 3d region (B). The peak of Fe 2p appears at 708.2 eV, which is characteristic of Fe(II) [46]. There is no evidence of Fe(III) existing in SmHCF samples, because the XPS peak corresponding to Fe(III) should appear at 710 eV [46]. The peak of Sm 3d appears at 1,082.7 eV (Fig. 4B), which corresponds to the characteristic peak of Sm(III). The Sm(II) peak should be at 1,074.0 eV [47].

Solid state electrochemistry

Figure 5a shows a typical cyclic voltammogram obtained when a paraffin-impregnated graphite electrode with mechanically attached $NaSmFe(CN)_6{\cdot}3H_2O$ was placed in a solution of 0.2-M NaCl at a scan rate of 100 mV/s. Figure 5b is a cyclic voltammogram of a bare graphite electrode. Those results indicate that a pair of well-defined redox peaks appearing on curve a can be ascribed to the redox reaction of $NaSmFe(CN)_6{\cdot}3H_2O$. The anodic and cathodic peak potentials are 213 and 148 mV, respectively, and the formal potential, $E^{0'}$, which was defined as the mid-point potential of the anodic and cathodic peak potentials, is 180.5 mV at a scan rate of 100 mV/s. The separation of the anodic and cathodic peak potentials, ΔE_p, is 65 mV. The electrochemical reaction process of the redox couple of curve a can be expressed as following:

$$NaSmFe^{II}(CN)_6 \rightarrow SmFe^{III}(CN)_6 + Na^+ + e^-(\text{in NaCl solution}) \quad (1)$$

It should be noted that the formal potential of SmHCF is more negative than that of transition metal hexacyanoferrates, such as cobalt hexacyanoferrate [10, 11, 29] and nickel hexacyanoferrate [27]. The same phenomenon was also found in the case of lanthanum hexacyanoferrate [4]. These differences might be caused by the different properties of transition and rate earth metal. However, the exact reason is not understood at present.

Figure 6 is the cyclic voltammograms of a paraffin-impregnated graphite electrode with attached $NaSmFe(CN)_6{\cdot}3H_2O$ obtained in 0.2-M NaCl solution at various scan rates. The values of $E^{0'}$ (181.2 ± 0.5 mV) and the ΔE_p (66.5 ± 2.5 mV) are almost independent on the scan rates in the range of 20 to 1,000 mV/s since the anodic and cathodic peak potentials hardly change with the increase of the scan rate. The cathodic and anodic peak currents are almost equal at all scan rates and both of them, not as expected, do not increase linearly with the scan rates (see inset A). However, the results of inset B to Fig. 6 show that both of cathodic and anodic peak currents do increase linearly with the square root of scan rates ($v^{1/2}$) up to as high as 1,000 mV/s, suggesting the reaction is not a surface-controlled process but a diffusion-controlled one [48]. It is generally accepted that the transfer of an electron is always accompanied by the simultaneous motion of a counter-cation, such as Na^+, K^+ and Li^+ ion etc., to maintain charge balance during

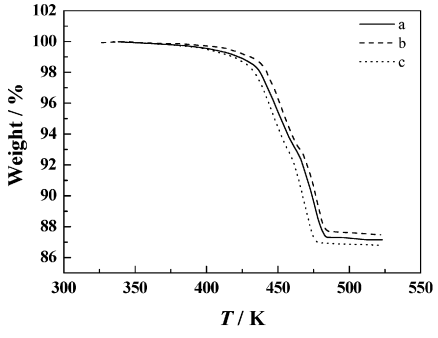

Fig. 2 The TGA curves of $KSmFe(CN)_6{\cdot}3H_2O$ (curve a), $NaSmFe(CN)_6{\cdot}3H_2O$ (curve b) and $LiSmFe(CN)_6{\cdot}3H_2O$ (curve c)

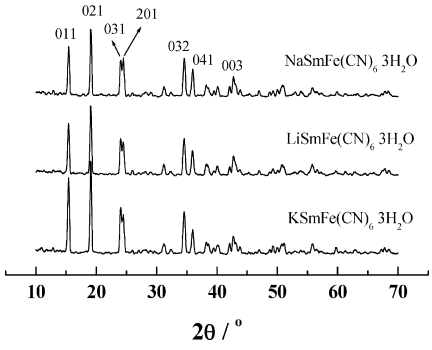

Fig. 3 The XRD patterns of SmHCF

Table 1 The lattice parameters of SmHCF

SmHCF	*a* (Å)	*b* (Å)	*c* (Å)
$LiSmFe(CN)_6{\cdot}3H_2O$	7.303 ± 0.019	13.680 ± 0.026	7.299 ± 0.013
$NaSmFe(CN)_6{\cdot}3H_2O$	7.284 ± 0.022	13.684 ± 0.026	7.262 ± 0.023
$KSmFe(CN)_6{\cdot}3H_2O$	7.290 ± 0.009	13.708 ± 0.012	7.262 ± 0.025
$SmKFe(CN)_6{\cdot}3H_2O$[a]	7.328	13.691	7.326

[a]The lattice parameters of this compound were taken from JCPDS card, file of 40-755

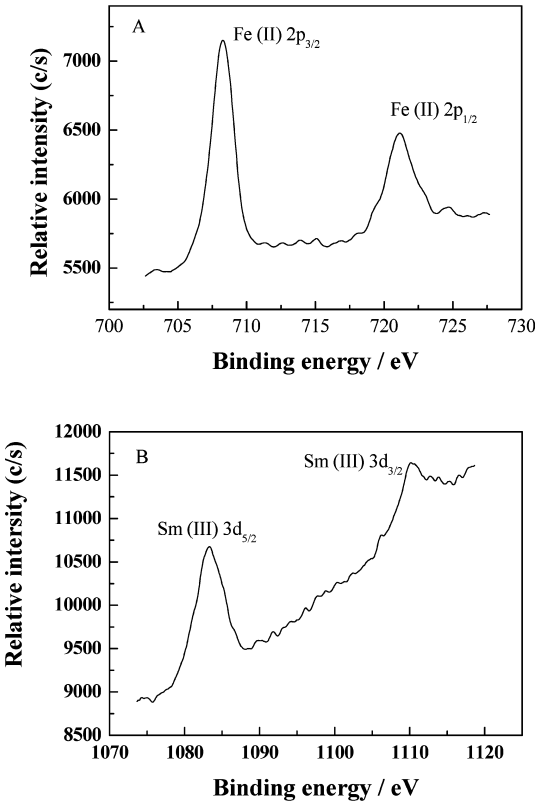

Fig. 4 XPS spectra of the Fe 2p region (**A**) and Sm 3d region (**B**) of SmHCF

the electrochemical reaction process of metal hexacyanoferrates [6, 10, 11, 12, 49]. The insertion of a counter-cation into the film during the reduction and its exclusion upon oxidation have been verified by Kulesza et al. [49] using the electrochemical quartz crystal microbalance (EQCM) technique in the case of hexacyanoferrates of cobalt and nickel. In the process of the redox reaction, the transfer of counter-cation (Na^+) in the ion channel of $NaSmFe(CN)_6{\cdot}3H_2O$ microparticle may control the overall reaction process.

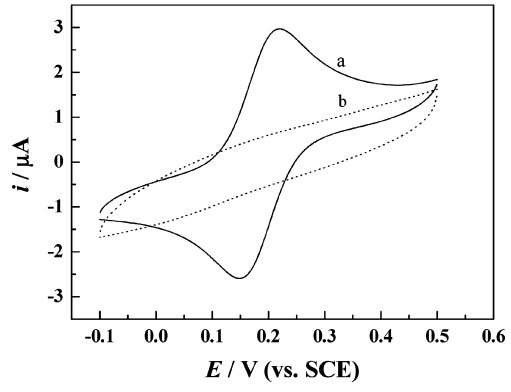

Fig. 5 Cyclic voltammograms of a graphite electrode with (curve a) and without (curve b) mechanically attached $NaSmFe(CN)_6{\cdot}3H_2O$ in the solution of 0.2-M NaCl at a scan rate of 100 mV/s

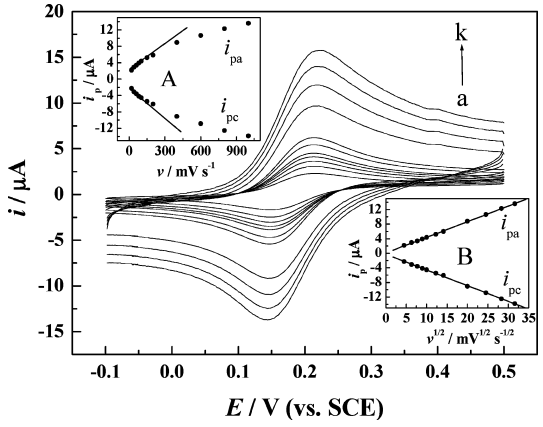

Fig. 6 Cyclic voltammograms of a graphite electrode attached $NaSmFe(CN)_6{\cdot}3H_2O$ in 0.2-M NaCl solution at a scan rate of (from curve a to k) 20, 40, 60, 80, 100, 150, 200, 400, 600, 800 and 1,000 mV/s, respectively. The inset shows the dependence of peak current on the scan rates (**A**) and the square root of the scan rates (**B**)

Figure 7 shows the cyclic voltammograms of a paraffin-impregnated graphite electrode with attached $NaSmFe(CN)_6{\cdot}3H_2O$ in NaCl solutions of different concentrations at a scan rate of 100 mV/s. It can be observed that both anodic and cathodic peak currents decrease and ΔE_p increases with the decrease in the concentration of NaCl. This indicates that the reversibility of the electrochemical reaction of the SmHCF increases with the increasing concentration of supporting electrolyte. The value of the formal potential moves linearly in a negative direction with decreasing NaCl concentration with a slope of 54.0 mV (for the plot of $E^{0'}$ versus $\log(c/\mathrm{M})$, where c is the concentration of supporting electrolyte, see the inset to Fig. 7), which is close to the theoretical value of 58.5 mV (at 22 °C) for a one-electron transfer process, indicating that the electrochemical reaction of SmHCF is accompanied by the transfer of an electron and an Na^+ ion (counter-cation).

Permeability towards counter-cations

It has been established that metal hexacyanoferrates show selective permeability towards the cations in the supporting electrolyte, such as alkali metal ions and other monovalent and divalent cations, due to their intrinsic zeolitic structure. Only those cations with hydrated radii smaller than that of the ion channel of hexacyanoferrates can be easily accommodated. The smaller the cation is, the more easily it passes [12].

Figure 8 compares the cyclic voltammetric responses of $NaSmFe(CN)_6{\cdot}3H_2O$ (curve a), $LiSmFe(CN)_6{\cdot}3H_2O$ (curve b) and $KSmFe(CN)_6{\cdot}3H_2O$ (curve c), which was mechanically attached to the surface of a graphite electrode, respectively, in the respective 0.2-M NaCl (a), LiCl (b) and KCl (c). From the cyclic voltammograms, one can see that the formal potential of SmHCF shifts slightly in the positive direction and the peak currents

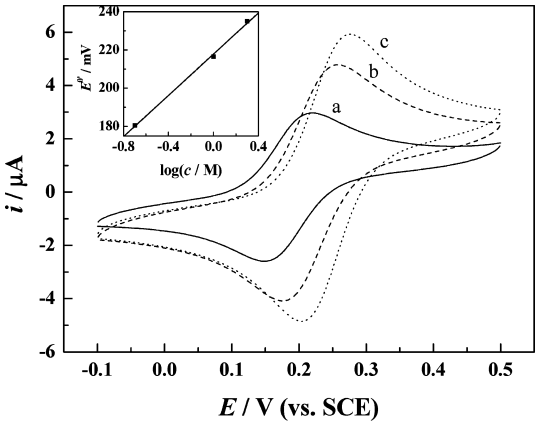

Fig. 7 Cyclic voltammograms of a graphite electrode attached $NaSmFe(CN)_6{\cdot}3H_2O$ in 0.2 (curve a), 1.0 (curve b) and 2.0-M (curve c) NaCl solution at a scan rate of 100 mV/s. The inset shows the dependence of the $E^{0'}$ on the concentration of supporting electrolyte

decrease drastically in the order of NaCl, LiCl and KCl. The decrease in peak currents cannot be due to a decrease in the amount of sample on electrode surface since similar conditions were applied each times when the samples were attached onto the surface of the electrode. Thus, the decrease in peak currents indicates the different permeability of SmHCF towards supporting cations and the permeability is in the order of $Na^+ > Li^+ > K^+$. From the peak currents, it seems that the Na^+ ion matches the ion channel of SmHCF the most closely and SmHCF possesses a prior selectivity for Na^+ ion as a counter-ion among the above three cations. This property of the SmHCF may be used for cation recognition.

The order of the permeability of SmHCF towards Na^+, Li^+ and K^+ is not consistent with that for most transition metal hexacyanoferrate. For example, PB shows permeability in the order of $K^+ > Na^+ > Li^+$

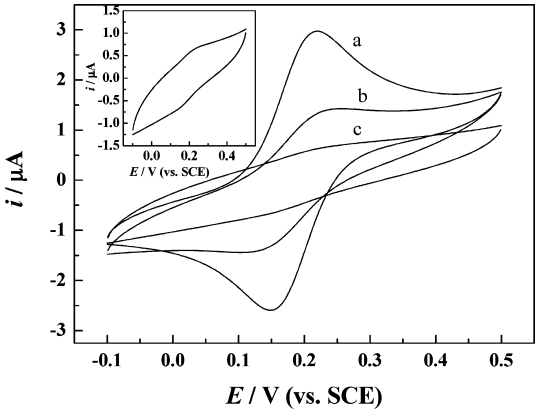

Fig. 8 Cyclic voltammograms of a graphite electrode attached $NaSmFe(CN)_6{\cdot}3H_2O$ (curve a), $LiSmFe(CN)_6{\cdot}3H_2O$ (curve b) and $KSmFe(CN)_6{\cdot}3H_2O$ (curve c), respectively, in the respective 0.2-M NaCl (curve a), LiCl (curve b) and KCl (curve c) solution at a scan rate of 100 mV/s. The inset shows the cyclic voltammogram of curve c on a different current scale

corresponding to the order of the radii of hydrated ions of Li^+, Na^+ and K^+ whose values are 0.12, 0.18 and 0.235 nm [50], respectively. Gao et al. [51] reported a permeability order of $K^+ > Na^+ > Li^+$ for CoHCF, and our previous results also indicated that the permeability order of CoHCF is $K^+ > Na^+ > Li^+$ [10, 11]. Engel et al. [52] reported the permeability order of CuHCF as $K^+ > Na^+$, and Kulesza et al. [53] and Dong et al. [54] showed the permeability order of InHCF is also $K^+ > Na^+$. These permeability orders are in accord with the order of hydrated ionic radius. However, Cui et al. [12] reported that the permeability of CuCoHCF towards supporting cations is in the order of $K^+ > Li^+ > Na^+$, which is not in accord with the order of hydrated ionic radius. Thus, the hydrated ionic radius of insertion ion is not exclusively the determining factor. The permeability of metal hexacyanoferrates towards counter-cations is such a complicated problem that there is a great difference in permeability among the hexacyanoferrates. Besides the radius of the cation, the major factors influencing the permeability of a cation also include the radius of the ion channel in hexacyanoferrates, the interactions between cations and hexacyanoferrates, including electrostatic interactions and ionic polarities, and the dehydration ability of the cation before it enters the channel of hexacyanoferrates [49] etc. To exclude the influence of the dehydration ability of cations on the permeability of SmHCF, it is helpful to carry out the experiments in non-aqueous solvents, which are currently being done, and we will report those results elsewhere.

Conclusions

A new rare earth metal hexacyanoferrate, samarium hexacyanoferrate (SmHCF), was prepared chemically in a solution of $SmCl_3$ and $Na_4Fe(CN)_6$ containing NaCl, LiCl or KCl as electrolyte, respectively, and characterized by the techniques of FTIR spectroscopy, thermogravimetric analysis (TGA), X-ray powder diffraction, UV–Vis spectrometry and X-ray photoelectron spectroscopy (XPS) etc. The solid state electrochemistry of SmHCF, which was mechanically attached to the surface of a graphite electrode, exhibited a pair of well-defined redox peaks with the formal potential of 180.5 mV (versus SCE) at a scan rate of 100 mV/s in 0.2-M NaCl solution and the redox peak currents increased linearly with the square root of the scan rate. The effect of the concentration of supporting electrolyte on the electrochemical characteristics of SmHCF and the transport behavior of K^+, Na^+ and Li^+ ions through the channel of SmHCF were studied. The voltammetric results showed a irregular permeability for the counter-cation in the order of $Na^+ > Li^+ > K^+$ and Na^+ ion matched the ion channel of SmHCF the most closely.

Acknowledgements The authors are grateful for the financial support of the National Natural Science Foundation of China

(20373027), the foundation for scientists returned from abroad directed under the State Ministry of Education of China, the Natural Science Foundation of Education Committee of Jiangsu Province (03KJA150055) and the Excellent Talent Project of Personnel Department of Nanjing City of Jiangsu Province.

References

1. Neff VD (1978) J Electrochem Soc 125:886
2. Itaya K, Ataka T, Toshima S (1982) J Am Chem Soc 104:3751
3. Karyakin AA (2001) Electroanalysis 13:813
4. Liu SQ, Chen HY (2002) J Electroanal Chem 528:190
5. Kulesza PJ, Malik MA, Schmidt R, Smolinska A, Miecznikowski K, Zamponi S, Czerwinski A, Berrettoni M, Marassi R (2000) J Electroanal Chem 487:57
6. Chen SM (2002) J Electroanal Chem 521:29
7. Xun ZY, Cai CX, Xing W, Lu TH (2003) Chin J Appl Chem 20:499
8. Pournaghi-Azar MH, Dastangoo H (2002) J Electroanal Chem 523:26
9. Razmi-Nerbin H, Pournaghi-Azar MH (2002) J Solid State Electrochem 6:126
10. Cai CX, Xue KH, Xu SM (2000) J Electroanal Chem 486:111
11. Xun ZY, Cai CX, Xing W, Lu TH (2003) J Electroanal Chem 545:19
12. Cui X, Hong L, Lin X (2002) J Electroanal Chem 526:115
13. Lezna RO, Romagnoli R, de Taccon NR, Rajeshwar K (2002) J Phys Chem B 106:3612
14. Bárcena Soto M, Scholz F, (2002) J Electroanal Chem 521:183
15. Vittal R, Gomathi H, (2002) J Phys Chem B 106:10135
16. Ricci F, Amine A, Palleschi G, Moscone D, (2003) Biosens Bioelectronics 18:165
17. de Mattos IL, Gorton L, Ruzgas T (2003) Biosens Bioelectronics 189:193
18. Malik MA, Miecznikowski K, Kulesza PJ (2000) Electrochim Acta 25:3777
19. Kelly MT, Arbuckle-Keil GA, Johnson LA, Su EY, Amos LJ, Chun JKM, Bocarsly AB (2001) J Electroanal Chem 500:311
20. Chen SM, Peng KT (2003) J Electroanal Chem 547:179
21. Monk PM, Mortimer RJ, Rosseinsky DR (1995) Electrochromism fundamentals and applications. VCH, Weinheim, Chapter 6
22. Kulesza PJ, Malik MA, Miecznikowski K, Wolkiewicz A, Zamponi S, Berrettoni M, Marassi R (1996) J Electrochem Soc 143: L10
23. Kertesz V, Dunn NM, Van Berkel GJ (2002) Electrochim Acta 47:1035
24. Lasky SJ, Buttry DA (1988) J Am Chem Soc 110:6258
25. Coon DR, Amos LJ, Bocarsly AB, Bocarsly PAF (1998) Anal Chem 70:3137.
26. Pournaghi-Azar MH, Razmi-Nerbin H, Hafezi B (2002) Electroanalysis 14:206
27. Cai CX, Ju JH, Chen HY (1995) Anal Chim Acta 310:145
28. Cai CX, Xue KH, Zhou YM, Yang H (1997) Talanta 44:339
29. Cai CX, Ju JH, Chen HY (1995) J Electroanal Chem 397:185
30. Mo JW, Ogorevc B, Zhang X, Pihlar B (2000) Electroanalysis 12:48
31. Golabi SM, Noor-Mohammadi F (1998) J Solid State Electrochem 2:30
32. Cataldi TRI, de Benedetto G, Bianchini A (1999) J Electroanal Chem 471:42
33. Ohkoshi S, Fujishima A, Hashimoto K (1998) J Am Chem Soc 120:5349
34. Sato O, Einaga Y, Iyoda T, Fujishima A, Hashimoto K (1997) J Phys Chem B 101:3903
35. Willems JJG (1984) Philips J Res 39:1
36. Zhao S, Sin JKO, Xu B, Zhao M, Peng Z, Cai H (2000) Sens Actuat B 64:83
37. Van Druten GMR, Labbé E, Paul-Boncour V, Périchon J, Percheron-Guéau A (2000) J Electroanal Chem 487:31
38. Jiang HJ, Huang XH, Wang XF, Li X, Xing W, Ding XL, Lu TH (2003) J Electroanal Chem 545:83
39. Wu P, Lu S, Cai CX J. Electroanal Chem (submitted)
40. Zakharchuk NF, Naumov N, Stösser R, Schröder U, Scholz F, Mehner H (1999) J Solid State Electrochem 3:264
41. Scholz F, Meyer B (1998) Voltammetry of solid microparticles immobilized on electrode surfaces. In: Bard AJ, Rubinstein I (ed) Electroanalytical chemistry, vol 20. Marcel Dekker, New York p 1
42. Scholz F, Lange B (1992) Trends Anal Chem 11:359
43. Dostal A, Meyer B, Scholz F, Schröder U, Bond AM, Marken F, Shaw SJ (1995) J Phys Chem 99: 2096
44. Ayers JB, Piggs WH (1971) J Inorg Nucl Chem 33:721
45. Xun ZY, Cai CX, Lu TH, Eletroanalysis (in press).
46. Cataldi TRI, de Benedtto GE, Bianchini AJ (1998) J Electroanal Chem 448:111
47. Mori K, Tanemura S, Koide S, Senzaki Y, Jin O, Kaneko K, Terai A, Nabotova-Gabin N (2003) Appl Surf Sci 212–213:38
48. Bard AJ, Faulkner LR (2001) Electrochemical method, fundamentals and applications, 2nd edn. Wiley, New York
49. Kulesza PJ, Malik MA, Berrettoni M, Giorgetti M, Zamponi S, Schmidt R, Marassi R (1998) J Phys Chem B 102:1870
50. Moelwyn-Hughes EA (1951) Physical chemistry. MacMillan, New York, p 589
51. Gao ZQ, Wang GQ, Li PB, Zhao ZF (1991) Electrochim Acta 36:197
52. Engel D, Grabner EW (1985) Ber Bunsenges Phys Chem 89:982
53. Kulesza PJ, Faszynska M (1988) J Electroanal Chem 252:461
54. Dong SJ, Jin Z (1989) Electrochim Acta 34:963